ELSEVIER

Carbohydrate Polymers 50 (2002) 393–406

Carbohydrate Polymers

www.elsevier.com/locate/carbpol

Dynamic rheology of agar gels: theory and experiments. Part I. Development of a rheological model

K.C. Labropoulos[a], D.E. Niesz[a], S.C. Danforth[a,*], P.G. Kevrekidis[b]

[a]*Department of Ceramic and Materials Engineering, Rutgers University, 607 Taylor Road, Piscataway, NJ 08854-8065, USA*
[b]*Department of Mathematics and Statistics, University of Massachusetts, Lederle Graduate Research Tower, Amherst, MA 01003-4515, USA*

Received 26 November 2001; revised 7 March 2002; accepted 8 March 2002

Abstract

A theoretical rheological model for agar gels is proposed, based on the bead and spring model for linear flexible random coils and the model for crosslinked polymers. The model introduces the concept of a temperature dependence of the monomeric friction coefficient, ζ_0, of the agar molecule. The model has a random coil-like behavior at high temperatures (close to 373 K), and contributions from a three-dimensional network at low temperatures (close to 273 K). A proposed temperature dependence of the net association rate allows the calculation of the fraction of associated molecules as a function of time and temperature. The proposed model predicts the gelation behavior of agar gels utilizing time–temperature data (cooling curves).

Keywords: Dynamic rheology; Agar gels; Flexible random coils

1. Introduction

Powder injection molding (PIM) is a low cost and high quality consolidation method that is used for the fabrication of complex shaped parts. Critical to the process is the introduction of a binder, which is mixed with a particulate material to impart the desired rheological properties to the feed mixture. Once the part is injection molded the binder phase needs to be removed prior to the final microstructural evolution of the powder. Often, the binder removal step imposes limitations on the shape complexity and size of the injection molded parts that can be made without shape distortion or cracking of the green parts (Lange, 1989). This is typical behavior of non-aqueous thermoplastic binder compositions used with PIM.

Various aqueous binder systems have been studied for use with PIM. Binders based on agar gels have shown the potential for fabrication of parts with large cross-sections, as well as extensive variations in thickness, within one part (Fanelli, Silvers, Frei, Burlew, & Marsh, 1989). These binders are environmentally benign and exhibit thermoplastic type rheological behavior.

Dynamic rheology has been used in the past to study the gelation behavior and the frequency dependence of the storage (G') and viscous (G'') moduli of agar gel based aqueous binders (Labropoulos, Rangarajan, Niesz, & Danforth, 2000; Labropoulos, Rangarajan, Niesz, & Danforth, 2001; Lai & Lii, 1997; Lai, Huang, & Lii, 1999; Lapasin & Pricl, 1995; Manno et al., 1999; Mohammed, Hember, Richardson, & Morris, 1998a; Norton, Jarvis, & Foster, 1999; Olhero, Tarì, Coimbra, & Ferreira, 2000; Tsoga, Kasapis, & Richardson, 1999). The mechanical behavior (Amici, Clark, Normand, & Johnson, 2000; Haga et al., 1998; Lee, Lee, & Song, 1997; Nitta, Haga, Kawabatta, Abe, & Sambongi, 2000; Normand, Lootens, Amici, Plucknett, & Aymard, 2000; Nussinovitch, Velez-Silvestre, & Peleg, 2001; Oates, Lucas, & Lee, 1993; Tsoga et al., 1999), microstructure (Amici et al., 2000; Charlionet, Levasseur, & Malandain, 1996; Griess, Guiseley, & Serwer, 1993a; Griess et al., 1993b; Kusukawa, Ostrovsky, & Garner, 1999) and structure–property relation (Manno et al., 1999; Pines & Prins, 1973; Ramzi, Rochas, & Guenet, 1998) of agar gels and their mixtures with other polymers have also been studied. While a number of phenomenological models have appeared in the literature (Lapasin & Pricl, 1995), these models are basically correlation equations and do not provide any insight at the microscopic or molecular scale.

Part I of this study discusses the development of a fundamental model that describes the rheological behavior of agar gels throughout the temperature range they encounter during injection molding. This model is based on rheological theories for dilute and crosslinked polymers. Part II of

* Corresponding author.
E-mail address: danforth@rci.rutgers.edu (S.C. Danforth).

0144-8617/02/$ - see front matter
PII: S0144-8617(02)00084-X

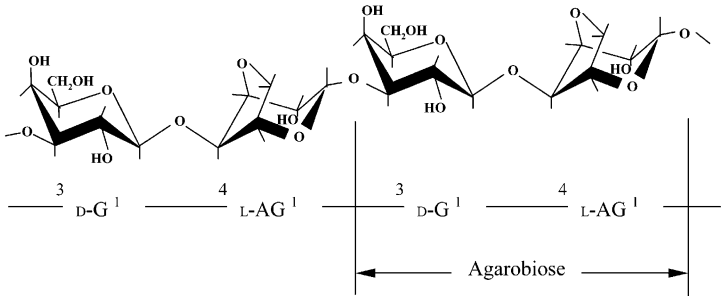

Fig. 1. The basic secondary structure of agar: D-G is β-D-galactopyranose and L-AG is 3,6 anhydro-α-L-galactopyranose. An agarobiose repeating unit is indicated (adapted from Araki (1956), Dea et al. (1972)).

this study discusses the dynamic rheology of agar gels and the proposed model is fitted to a wide range of experimental gelation curves.

2. Theoretical background

2.1. Structure of agar gels

2.1.1. Chemical composition of agar

Agar is a gel-forming polysaccharide with a sugar skeleton consisting of alternating 1,3-linked β-D-galactopyranose and 1,4-linked 3,6 anhydro-α-L-galactopyranose units (Araki, 1956; Arnott et al., 1974; Dea, McKinnon, & Rees, 1972; Harris, 1990; Hickson & Polson, 1968; Rees, 1972; Whistler & BeMiller, 1973). Agarobiose, the basic disaccharide structural unit of all agar polysaccharides is shown in Fig. 1. Agar can be fractionated into two components (Araki, 1944a,b; Araki, 1956; Araki & Hirase, 1954; Arnott et al., 1974; Dea et al., 1972; Hickson & Polson, 1968; Hirase, 1957; Rees, 1972). The fraction with the greatest gelling capability is termed agarose and is a neutral polysaccharide. The remaining fraction is termed agaropectin and contains all the charged polysaccharide components.

In agaropectin, however, some residues have been replaced by pyruvic acid ketal, 4,6-*O*-(1-carboxyethylidene) D-galactopyranose or by methylated or sulphated sugar units (Arnott et al., 1974; Falshaw, Furneaux, & Stevenson, 1998; Guiseley, 1970; Harris, 1990; Hirase, 1957). Depending on the seaweed source, the agarose and agaropectin contents will vary, affecting the physicochemical, mechanical and rheological properties of agar.

2.1.2. Tertiary and quaternary structure of agar

The microstructural, mechanical and rheological properties of agar gels can be described by a 'crosslinked network' model (Aplin & Hall, 1979; Arnott et al., 1974; Dea & Rees, 1987; Dea et al., 1972; Rees, 1972; Schafer & Stevens, 1995). In this model, a gradual change from a homogeneous aqueous sol to an elastic and turbid gel network occurs during cooling. This transformation is reversible but path dependent (i.e. exhibits hysteresis).

In the sol state, at temperatures close to the boiling point of water, the agar molecules take on a random coil conformation and are homogeneously distributed throughout the sol volume (Rees, 1972; Serwer, 1983). Gelation occurs by cooling the agar sol to a temperature below the gelation point. In the gel state, agar molecules are associated with each other forming a three-dimensional network. In the widely accepted *double helix* model, the basic structural unit is the double helix. Each chain (with an average molecular weight estimated to be 120,000, or about 390 agarobiose units (Arnott et al., 1974; Hickson & Polson, 1968)) forms a left-handed threefold helix of 1.9 nm pitch and is translated axially, relative to its partner, by 0.95 nm (Arnott et al., 1974; Dea et al., 1972). However, single chains (Schafer & Stevens, 1995) and other crystalline allomorphs (Kouwijzer & Pérez, 1998) have been reported in the literature.

Dea, Fulmer, and Scott (Arnott et al., 1974) have argued that the interior cavity, which extends along the length of the helix axis, is large enough to contain water molecules. The presence of bound water inside the double helix cavity has been verified by ^{1}H-NMR relaxation studies (Gabrielson & Edirisinghe, 1996) and adds to the stability of the double helix (Arnott et al., 1974).

Three of the four hydroxy groups ($O_{(2)}$, $O_{(4)}$, $O_{(6)}$ from the 3,6-anhydrogalactose) are pointing outwards and are engaged in hydrogen bonding with the bulk water molecules or neighboring helices. These hydrogen bonding interactions allow for the aggregation of double helices into higher order assemblies termed *suprafibers*. These assemblies may contain up to 10^4 double helices and contribute significantly to the elastic properties of the three-dimensional network (Arnott et al., 1974; Dea et al., 1972; Rees, 1972). As the stiffness of the double helix increases, its conformational entropy term (that favors dissolution in the solvent) is minimized (Arnott et al., 1974). Accordingly, the stiffness of the suprafibers, and subsequently the elastic and rheological properties of the gel network, will be dependent on the cohesion within and between double helices.

Substitutions on the basic secondary structure introduce steric limitations in double helix formation. Consequently, certain parts of the agar molecule are incompatible with double helix formation. These parts are termed *kinks* and lead to partner switching during association. Typically, agar

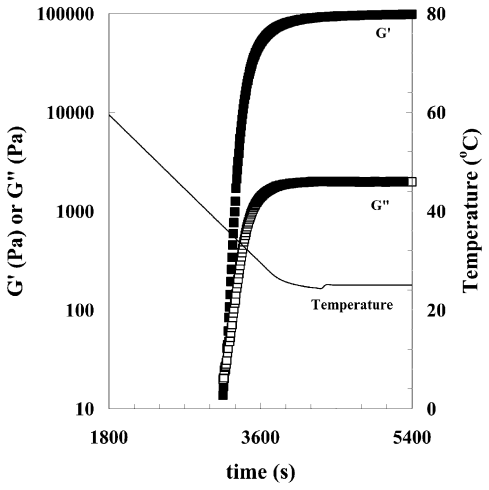

Fig. 2. Dynamic storage modulus, G' and dynamic viscous modulus, G'', vs. time of a 3 wt% agar sol on cooling from 90 to 25 °C at 1 °C min^{-1}. $t = 0$ at 90 °C during cooling, $\gamma = 1\%$, $\omega = 100$ rad s^{-1}, 25 mm parallel disk geometry.

molecules participate in more than one double helix. It should be noted that crosslinking in the traditional meaning of the term is actually not present. After the end of the gelation, each agar molecule is still discrete in the three-dimensional network and in principle can be separated without breaking any chemical bonds.

2.1.3. Molecular weight and double helix formation of agar gels

As mentioned above, agar consists of two fractions: agarose and agaropectin. The molecular weight of agar is rather variable and depends on the seaweed species it was extracted from. Thus, the $\overline{MW}$ of 120,000 in the literature (Hickson & Polson, 1968; Serwer, 1983) refers only to the agarose fraction. Agarose is monodispersed only after special preparation. Due to substitutions, the $\overline{MW}$ of agar is typically higher (up to 250,000) and has a wide distribution (Mitsuiki, Mizuno, & Motoki, 1999), while its gelling behavior is typically less effective than that of agarose.

In the literature, (Aplin & Hall, 1979; Arnott et al., 1974; Dea et al., 1972; Hickson & Polson, 1968; Rees, 1972) no supporting evidence is presented on how the agarose double helices align inside the suprafibers. Although crystalline allomorphs have been predicted (Kouwijzer & Pérez, 1998), where rigid helices pack in a distinct pattern to form crystals, their presence in the typical gelating conditions employed throughout most of the studies is questionable. In general, it is assumed (or presented in schematics) that the double helices align parallel to the suprafiber axis (Arnott et al., 1974; Rees, 1972; Serwer, 1983). This is most probably true for very low concentrations of agarose (where the suprafibers may contain only a few double helices) or for agar gel networks where the suprafibers are thin in diameter and short in length. However, the probability of having the same packing efficiency for the highly substituted agar molecules at the concentrations (up to 20 wt%) and cooling rates (higher than 60 °C min^{-1}) used in PIM may be lower.

2.2. Gelation temperature

The gelation temperature, T_{gel}, characterizes the transition from a liquid-like sol, to a solid-like gel phase. Throughout the literature, various methods have been used to estimate T_{gel}. The 'sedimentation of glass beads' is the most common method (Dea & Rees, 1987; Dea et al., 1972; Falshaw et al., 1998; Guiseley, 1970; Kusukawa et al., 1999), in which glass beads are introduced on the surface of a cooling sol, and the temperature at which they fail to sink is described as T_{gel} (more correctly termed setting temperature). Although this method is simple, it effectively provides the temperature (herein termed T_{onset}^{beads}) at which a macroscopic network is sufficiently strong to support the weight of a glass bead. This method is typically used for quality control of the resultant gel. In general, the higher the setting temperature of the sol, the more rigid the resultant gel will be (Harris, 1990).

Another approach is to define T_{gel} as the temperature during cooling when $\tan\delta = G''/G' = 1$ (Lai & Lii, 1997; Lai et al., 1999; Tsoga et al., 1999), where G' and G'' are the dynamic moduli of the sol. This temperature, often termed T_g, is not easily measurable, since most rheometers are not adequately sensitive to allow direct observation of the G'–G'' crossover. Due to the complex nature of the temperature dependence of G' and G'' at the early stages of gelation (Manno et al., 1999), extrapolating the moduli vs. temperature curves may not be accurate.

An alternative approach is to define T_{gel} as the temperature, where the onset of gelation occurs. The onset of gelation can be observed either by dynamic rheology (Labropoulos et al., 2001; Mohammed et al., 1998a) or by optical rotation measurements (Arnott et al., 1974; Dea & Rees, 1987; Dea et al., 1972; Mohammed et al., 1998a). In the first case, the onset of gelation, T_{onset}, is described by a very steep rise in the temperature dependence of the dynamic moduli (Fig. 2). Often though, T_{onset} is limited by instrument resolution. Instead, the gelation temperature is defined as the temperature (herein termed $T_{onset}^{modulus}$) at which a certain value of modulus, e.g. $G' = 1$ Pa, is reached (Labropoulos et al., 2001; Mohammed et al., 1998a).

In optical rotation measurements, the gelation point is defined as the temperature (herein termed $T_{onset}^{optical}$), where the specific rotation changes rapidly. Spectroscopic type measurements essentially evaluate the conformational changes associated with the sol–gel transition, rather than the formation of a rigid network. Therefore, this method can identify the coil-to-helix transitions at higher temperatures than the previous methods. However, such transitions may not necessarily correspond to the formation of a macroscopic three-dimensional gel network.

In general, the gelation temperature obtained by the method of sedimentation of beads, T_{onset}^{beads}, is lower than the gelation temperature obtained by observation of the

onset of gelation through dynamic rheology, $T_{onset}^{modulus}$.. In turn, $T_{onset}^{modulus}$ is lower than the gelation temperature obtained for $\tan\delta = 1$, T_g. Finally, T_g is lower than the gelation temperature obtained by observation of the onset of gelation through optical rotation experiments, $T_{onset}^{optical}$ (Mohammed et al., 1998a). Normally, the gelation temperature of agarose increases with increasing methoxyl content (Guiseley, 1970) and increases with slower cooling rates (Harris, 1990). Typical values for T_{gel} range from 28 to 50 °C and depend on the origin of the agar used (Harris, 1990).

For the development of a rheological model for agar gels, we define T_{gel}^{model} as the temperature during cooling of an agar sol, above which any associated agar molecules cannot form a continuous three-dimensional network. This definition is related to the kinetic and equilibrium processes that take place during gelation. For any cooling history, if the temperature is held below T_{gel}^{model}, eventually a rigid agar network will form. A similar approach has appeared in the literature by considering the temperature dependence of the initial rates of gelation (approximated by the inverse of the time to reach a certain value of modulus when held at a certain temperature) and extrapolating to zero (Mohammed et al., 1998a). The same approach will be followed here, to provide a first estimate of T_{gel}^{model}.

2.3. Existing models for polymers and their applicability to agar gels

It is difficult to describe the viscoelastic behavior of agar gels with just one polymer model. On one hand, at high temperatures, the rheological behavior of agar sols is similar to dilute solutions of linear polymers. On the other hand, at low temperatures below the gelation point, their behavior is similar to that of crosslinked polymers. In the temperature range where the sol–gel transition occurs, the situation is further complicated by the fact that polymerization is not occurring in the traditional sense of the term (i.e. permanent chemical bonding between monomers). Instead, realignment, physical entanglements and reversible association (hydrogen bonding) of discrete macromolecules result in the formation of a three-dimensional network. This sol–gel transition has a hysteretic behavior (Labropoulos et al., 2001; Mohammed et al., 1998a). Also, as will be discussed later, the rheological properties of agar gels depend on thermal history. Nonetheless, since the existing rheological models will form the basis for the development of a model suited for agar gels, their range of applicability should be studied.

2.3.1. Bead spring models for linear flexible random coils

The simplest example of polymer systems, which is applicable for agar gels in their sol state, is a dilute solution of a linear flexible polymer. As indicated in the literature, at high temperatures (close to 100 °C) in the sol state, agar molecules take on a random coil conformation (Arnott et al., 1974; Dea et al., 1972; Rees, 1972). It is theorized that agar sols can be described by the bead spring models developed for linear flexible random coils.

In these models, the flexible polymer molecule is represented by N submolecules (each containing q monomers) joining $N + 1$ identical beads with complete flexibility at each bead (Rouse, 1953; Zimm, 1956). Each submolecule is a portion of the polymer chain, just long enough so that the root-mean-square end-to-end length of the submolecule, σ, obeys to a first approximation, a Gaussian probability function. Fluctuations in the length of the submolecule result in an entropy change of the system, associated with imposed restrictions on the number of conformations that can be attained (Rouse, 1953; Zimm, 1956).

The introduction of the beads simplifies the problem since it is assumed that the chain interacts with the liquid through the beads only. According to the theories of Rouse (1953) and Zimm (1956), when a dilute solution of polymer molecules is subjected to shear, the interaction of the jth bead with its surroundings consists of a force with components F_{xj}, F_{yj}, F_{zj}. The force is proportional to the velocity of the bead moving in the liquid (Zimm, 1956):

$$F_{xj} = f_0(\dot{x}_j - u'_{xj}) \tag{1a}$$

$$F_{yj} = f_0(\dot{y}_j - u'_{yj}) \tag{1b}$$

$$F_{zj} = f_0(\dot{z}_j - u'_{zj}) \tag{1c}$$

where f_0 is the friction coefficient of the submolecule, $\dot{x}_j, \dot{y}_j, \dot{z}_j$ and $u'_{xj}, u'_{yj}, u'_{zj}$ are the velocity components that the fluid has with and without the presence of the bead, respectively.

This interaction force is combined with the Brownian motion of the molecules and the force due to the perturbation of the length of the Hooke's law spring-like molecular segments to provide the equations of motion. The equations of motion are then transformed into a set of differential equations and solved accordingly. More details can be found in the original literature (Bueche, 1952; Rouse, 1953; Tsoegl, 1963; Zimm, 1956).

2.3.2. Rouse theory

The two main theories (Rouse's and Zimm's) differ mainly on how hydrodynamic interactions between the molecule and the solvent are taken into account. In the Rouse theory, a 'free-draining' approximation assumes that the polymer molecule does not distort the flow lines in the solvent (Bueche, 1952; Rouse, 1953). With this assumption, the Rouse theory gives the following results:

$$[G']_R = \sum_{p=1}^{N} \omega^2 \tau_p^2 / \left(1 + \omega^2 \tau_p^2\right) \tag{2}$$

$$[G'']_R = \sum_{p=1}^{N} \omega \tau_p / \left(1 + \omega^2 \tau_p^2\right) \tag{3}$$

$$\tau_p = \frac{\sigma^2 q \zeta_0}{24kT \sin^2 [p\pi/2(N+1)]} \quad (4)$$

where $[G']_R = M/RT \lim_{c\to 0} G'/c$ is the reduced intrinsic storage modulus, $[G'']_R = M/RT \lim_{c\to 0} (G'' - \omega\eta_s)/c$ is the reduced intrinsic loss modulus, c is the polymer concentration, M is the polymer molecular weight, τ_p is a relaxation time, ζ_0 is the monomeric friction coefficient (assuming that an average value can be used for all junctions; $\zeta_0 = f_0/q$, where f_0 is the friction coefficient of the submolecule and q is the number of monomers per submolecule), N is the number of submolecules, T is the temperature, ω is the frequency of the applied oscillatory deformation and p is an index number.

If the main contribution to the moduli comes from those relaxation times, τ_p, for which $p < N/5$, the Rouse theory indicates that Eq. (4) can be simplified to(Ferry, 1980; Larson, 1988; Rouse, 1953):

$$\tau_p = \frac{\sigma^2 N^2 f_0}{6\pi^2 p^2 kT} = \frac{\alpha^2 P^2 \zeta_0}{6\pi^2 p^2 kT} = \frac{S^2 P \zeta_0}{6\pi^2 p^2 kT} = \frac{6[\eta]\eta_s M}{\pi^2 p^2 RT} \quad (5)$$

where it is assumed that $\sigma = \alpha\sqrt{q}$ (the length α depends on local parameters), and the mean square separation of the ends of the whole molecule is $S^2 = \alpha^2 P$, where P is the degree of polymerization of the polymer chain. In addition, as shown in Eq. (5), the Rouse relaxation spectrum can be estimated by experimentally observable quantities such as the intrinsic viscosity, $[\eta]$, the solvent viscosity, η, and the molecular weight, M. In both cases, the approximation for the relaxation times given by Eq. (5), does not contain any factors dependent upon the length of the 'artificial' submolecules.

At finite concentrations sufficiently small that $[G']_R$ can be approximated by $G'M/cRT = G'/nkT$ where c is the polymer concentration and n is the number of polymer molecules per unit volume, Eqs. (2) and (3) become (Ferry, 1980; Rouse, 1953):

$$G' = nkT \sum_{p=1}^{N} \omega^2 \tau_p^2 / \left(1 + \omega^2 \tau_p^2\right) \quad (6)$$

$$G'' = \omega\eta_s + nkT \sum_{p=1}^{N} \omega\tau_p / \left(1 + \omega^2 \tau_p^2\right) \quad (7)$$

The use of the submolecule as the fundamental relaxing unit does not take into account relaxation processes from segments of the chain smaller than the submolecule. These processes occur faster than the processes involving coordination of longer chain segments and correspond to short relaxation times. The contributions to the viscoelastic functions of these fast processes is negligible at low frequencies, but increase above $\omega_{\tau 1} > 0.1$. This is the upper limit of applicability of the theory. At higher frequencies, both $[G']_R$ and $[G'']_R$ are equal and proportional to $\omega^{1/2}$ (Ferry, 1980; Larson, 1988; Rouse, 1953).

2.3.3. Zimm theory

In the theory of Zimm, the hydrodynamic interaction between the molecule and the solvent affects the eigenvalues of the solution of the equations of motion through a parameter h, that measures the strength of the hydrodynamic interaction (Ferry, 1980; Larson, 1988; Tsoegl, 1963; Zimm, 1956). In the case, where $h = 0$, the Zimm theory reduces to the Rouse theory (Zimm, 1956). For other values of h, the solutions to the equations of motion lead to a discrete spectrum that differs from that of Rouse theory only in the spectrum of relaxation times obtained. Thus, Eqs. (2) and (3) are unchanged. The Zimm theory predicts a slightly different spectrum of relaxation times with an $\omega^{2/3}$ dependence of the reduced moduli at the high frequency region. More detailed discussion on the interaction parameter h can be found in the original literature (Bueche, 1952; Tsoegl, 1963; Zimm, 1956). For partial hydrodynamic interaction, where the parameter h takes values between zero (Rouse model) and infinity (Zimm model) the reader is directed to the work of Tsoegl (1963).

2.3.4. Rigid elongated molecules

A number of theories have been developed for dilute solutions of elongated rod-like macromolecules (Kirkwood & Auer, 1951; Ookubo, Komatsubara, Nakajima, & Wada, 1976; Ullman, 1969; Warren, Schrag, & Ferry, 1973; Yamakawa, 1975). Rigid elongated molecules will have a finite intrinsic viscosity, $[\eta]$, and a reduced viscous modulus, $[G'']_R$, due to dissipation of energy when an oscillatory shear field is applied. When no shear is applied, the distribution of orientations of the rod-like molecules will be random. This distribution, though, changes during the cycle of an oscillatory shear field and the resulting decrease in entropy corresponds to storage of elastic energy. Generally, these models predict the existence of an end-to-end rotation relaxation time, τ_0, and the viscoelastic functions can be generalized as follows (Ferry, 1980; Lapasin & Pricl, 1995):

$$[G']_R = \frac{m_1 \omega^2 \tau_0^2}{1 + \omega^2 \tau_0^2} \quad (8)$$

$$[G'']_R = \omega\tau_0 \left(\frac{m_1}{1 + \omega^2 \tau_0^2} + m_2 \right) \quad (9)$$

$$\tau_0 = \frac{[\eta]\eta_s M}{(m_1 + m_2)RT} \quad (10)$$

where m_1 and m_2 are coefficients that depend on the model (Ferry, 1980).

The main feature of these rod-like models that is important for agar gels is the prediction of an end-to-end rotation relaxation time (Eq. (10)). Such a rotational mode relaxation time can be related to the relaxation behavior of agar entities (*clusters*) present above the gelation temperature, T_{gel}^{model}, as will be discussed later.

2.3.5. Partially flexible helical macromolecules

Helical polysaccharide macromolecules typically exhibit some degree of stiffness (Lapasin & Pricl, 1995; Yamakawa & Fujii, 1973). Therefore, the theories developed for flexible random coils or rigid molecules cannot be used without appropriate modifications. The worm-like chain model of Kratky and Porod (1949) describes the characteristic parameters of helical molecules. Specifically, the stiffness of the molecule is related to a parameter termed persistence length q (not to be confused with the number of monomers per submolecule appearing in Eq. (4)), which is the average projection of the end-to-end vector of an infinitely long molecule onto the tangent vector at the chain end (Ferry, 1980; Lapasin & Pricl, 1995; Yamakawa & Fujii, 1973). If the contour length, L, of the helix is comparable to q, then the helix behaves like a rigid rod. If the contour length of the helix is much larger than the persistence length, then the behavior approaches that of a random coil.

When the stiffness of the molecule is increased, the terminal relaxation time, τ_1, is becoming larger and separated from the others (Bixon & Zwanzig, 1978a). An alternative hybrid relaxation spectrum was used by Warren et al. (1973) to describe the viscoelastic behavior of helical polymers. The model includes a separate rotational mode relaxation time, τ_0, that is added to the relaxation spectra as predicted by Zimm theory:

$$[G']_{\mathrm{R}} = \frac{m_1 \omega^2 \tau_0^2}{1 + \omega^2 \tau_0^2} + zZ'(\omega\tau_1) \tag{11}$$

$$[G'']_{\mathrm{R}} = \omega\tau_0 \left(\frac{m_1}{1 + \omega^2 \tau_0^2} + m_2 \right) + zZ''(\omega\tau_1) \tag{12}$$

where

$$Z'(\omega\tau_1) = \sum_{p=1}^{N} \frac{(\omega\tau_1)^2 (\tau_p/\tau_1)^2}{1 + (\omega\tau_1)^2 (\tau_p/\tau_1)^2} \tag{13}$$

$$Z''(\omega\tau_1) = \sum_{p=1}^{N} \frac{(\omega\tau_1)(\tau_p/\tau_1)}{1 + (\omega\tau_1)^2 (\tau_p/\tau_1)^2} \tag{14}$$

where the ratios τ_p/τ_1 are given by the Zimm theory. The addition of a rotational mode relaxation time has been adopted in the proposed rheological behavior of the agar entities before the formation of a three-dimensional network.

2.3.6. Molecular theories for networks and entanglements

The effect of entanglements or crosslinks to the dynamic moduli is to introduce an 'equilibrium' shear modulus, G_{e}, at infinitesimal deformations, as predicted by rubber elasticity: (Ferry, 1980; Flory, Hoeve, & Ciferri, 1959; Mooney, 1959; Tobolsky, Carlson, & Indictor, 1961)

$$G_{\mathrm{e}} = \left(\frac{\overline{r_i^2}}{\overline{r_f^2}} \right) \nu kT = \Phi \nu kT \tag{15}$$

where $\overline{r_i^2}$ is the mean square end-to-end distance of a strand, $\overline{r_f^2}$ is the mean square end-to end distance of a strand not constrained by crosslinks, and ν is the number of strands per unit volume. The factor $\Phi = \overline{r_i^2}/\overline{r_f^2}$ is taken as unity for ideal rubbery polymers (Ferry, 1980).

Mooney (1959) has studied the viscoelastic properties of rubbery polymers and found that the relaxation spectrum is similar to that of an undiluted polymer with the addition of a term corresponding to the equilibrium modulus G_{e}:

$$G' = \nu kT \left[\Phi + \sum_{p=1}^{N} \omega^2 \tau_p^2 / \left(1 + \omega^2 \tau_p^2 \right) \right] \tag{16}$$

$$G'' = \nu kT \sum_{p=1}^{N} \omega\tau_p / \left(1 + \omega^2 \tau_p^2 \right) \tag{17}$$

$$G(t) = \nu kT \left[1 + \sum_{p=1}^{N} \mathrm{e}^{-t/\tau_p} \right] \tag{18}$$

$$\tau_p = \frac{\sigma^2 N^2 f_0}{6\pi^2 p^2 kT} = \frac{\alpha^2 P_{\mathrm{s}}^2 \zeta_0}{6\pi^2 p^2 kT} = \frac{S^2 P_{\mathrm{s}} \zeta_0}{6\pi^2 p^2 kT} \tag{19}$$

where $P_{\mathrm{s}} = \rho/\nu M_0$ is the degree of polymerization of the strand, ρ is the density of the polymer, M_0 is the monomeric molecular weight and the remaining parameters have been described in Eqs. (4) and (5). Tobolsky et al. (1961) debate that the factor $\Phi = (\overline{r_i^2}/\overline{r_f^2})$ should always appear in the equilibrium modulus (as has been done in Eq. (16)) since it may not be unity even for ordinary rubber networks.

This factor, Φ, is also important for agar gels, since the root mean square end-to-end length of the agar molecules, S, obviously does not obey a Gaussian probability function when the molecules are associated (at low temperatures) to form higher order assemblies such as double helices and suprafibers. This factor, Φ, will be indicative of the enhanced equilibrium modulus of the agar network due to the presence of the double helices and suprafibers (which theoretically have a much lower compliance than a random coil).

3. Development of a rheological model for agar gels

3.1. Rheological behavior of the non-associated agar molecules

It is theorized that the rheological behavior of the non-associated agar molecules, in the high temperature range, can be described by the theories developed for dilute polymers. In particular, at temperatures in the vicinity of 100 °C, agar molecules are expected to have a random coil conformation. Thus, their rheological behavior could be described by the Rouse theory (Eqs. (2)–(7)), assuming the solvent–molecule hydrodynamic interaction is minimal ($h = 0$).

As the temperature is lowered, the hydrodynamic

interaction parameter, h, may increase. The relaxation spectrum will then tend to shift from that predicted by the Rouse theory ($h = 0$) to that predicted by the Zimm theory ($h = \infty$). According to the Rouse model, the relaxation times of random coils are inversely proportional to the absolute temperature (Eq. (5)). The parameters σ, S, f_0, α, and ζ_0 (Eq. (4)) are also temperature dependent, because the surroundings and conformations of the agar molecules change significantly during cooling, especially in the vicinity of the gelation temperature. Accordingly, the exact temperature dependence of the relaxation times is expected to be complex.

The monomeric friction coefficient, $\zeta_0(T)$, should increase as the temperature is lowered. The friction forces encountered by the beads are higher mainly due to chemical interactions from the presence of a developing network. The friction forces are also higher due to the increased viscosity of the solvent. Although, strictly speaking, the Zimm model (Zimm, 1956) describes the behavior of dilute polymers with dominant hydrodynamic interaction, as explained above, the Rouse model (Rouse, 1953) should be sufficient for the purpose of this study.

The difference between the spectra predicted by the Rouse and Zimm theories are relatively small (Ferry, 1980). Most of the increase in the contributions from the non-associated molecules will occur because the relaxation times themselves will shift towards higher values (due to a change in S, T and ζ_0) and not because of the increased hydrodynamic factor (i.e. going from a Rouse-like behavior, $h = 0$ to a Zimm-like behavior, $h = \infty$). The monomeric friction coefficient should increase as the temperature is lowered and should tend to infinity at the freezing point (assuming there exist any free molecules at that temperature). An empirical temperature dependence that describes such a behavior is the following:

$$\zeta_0(T) = \zeta_{\mathrm{HT}}\left(\frac{T_{\mathrm{ref}} - T_{\mathrm{low}}}{T - T_{\mathrm{low}}}\right)^{A_2} \tag{20}$$

where ζ_{T} is the high temperature limit of $\zeta_0(T)$, T_{ref} is an arbitrary reference temperature (373.15 K), T_{low} is a temperature that signifies the decreased *mobility* of the agar molecules as the freezing point is approached ($T_{\mathrm{low}} =$ 273.15 K), T is the absolute temperature (K) and A_2 is a power exponent that dictates how the transition of $\zeta_0(T)$ from ζ_{HT} to ∞ occurs.

Since $S(T)$, and $\zeta_0(T)$ both change with temperature, for simplicity, any changes in the $S(T)$ can be lumped into the $\zeta_0(T)$ term. Thus, only a value S_{ref} needs to be known, taken at a reference temperature, T_{ref}, in the high temperature region and above the gelation temperature. Then the proposed equation for the relaxation times becomes:

$$\tau_p = \frac{S_{\mathrm{ref}}^2 P \zeta_{\mathrm{HT}}}{6\pi^2 p^2 kT}\left(\frac{T_{\mathrm{ref}} - T_{\mathrm{low}}}{T - T_{\mathrm{low}}}\right)^{A_2} \tag{21}$$

In the above equation, we set $\tau_1^{\mathrm{ref}} = S_{\mathrm{ref}}^2 P \zeta_{\mathrm{HT}}/6\pi^2 k T_{\mathrm{ref}}$. τ_1^{ref} is the terminal relaxation time of the random coiled agar molecules at an arbitrary reference temperature T_{ref} in the high temperature range (example, $T_{\mathrm{ref}} = 370$ K). This is introduced only to make the constant τ_1^{ref} have units of time. Eq. (21) then becomes:

$$\tau_p = \frac{\tau_1^{\mathrm{ref}} T_{\mathrm{ref}}}{p^2 T}\left(\frac{T_{\mathrm{ref}} - T_{\mathrm{low}}}{T - T_{\mathrm{low}}}\right)^{A_2} \tag{22}$$

3.2. Association processes of agar molecules

The definition of $T_{\mathrm{gel}}^{\mathrm{model}}$ (Section 2.2) does not rule out the association of agar molecules above $T_{\mathrm{gel}}^{\mathrm{model}}$. In particular, a cluster is defined as a group of associated agar molecules that exist in any kind of conformation (including helical), where each molecule is associated with at least one other partner to form any kind of entanglements.

This concept of clusters is in good agreement with the model of agarose gel formation, which has been proposed to be a combination of spinodal demixing, molecular conformational changes and entangling processes. (Bulone, Emanuele, & San Biagio, 1999; Lapasin & Pricl, 1995; Manno et al., 1999) The presence of clusters has also been verified by dynamic rheology using thixotropic loop experiments to observe the presence of association at temperatures above the onset of gelation (Cesarano, 1989).

It should be noted that clusters may exist even above $T_{\mathrm{gel}}^{\mathrm{model}}$. However, since they are unconnected, the sol has still a liquid-like behavior. Consequently, if the temperature is held slightly above $T_{\mathrm{gel}}^{\mathrm{model}}$, no continuous three-dimensional network should appear, even after infinite time. Effectively, at temperatures above $T_{\mathrm{gel}}^{\mathrm{model}}$ there exists an equilibrium between the number of agar molecules associated in clusters, $n_{\mathrm{clusters}}(T)$, and the number of 'free' agar molecules in the agar sol, $n_{\mathrm{free}}(T)$:

$$n_{\mathrm{free}}(T) \overset{T>T_{\mathrm{gel}}}{\leftrightarrow} n_{\mathrm{clusters}}(T) \tag{23}$$

When the temperature drops below $T_{\mathrm{gel}}^{\mathrm{model}}$, a driving force for gelation develops, that is proportional to the degree of undercooling, $\Delta T = T_{\mathrm{gel}}^{\mathrm{model}} - T$. Higher values of ΔT yield enhanced gelation kinetics at the initial stages of gelation (Mohammed et al., 1998a). Subsequently, a continuous three-dimensional network will develop with time. At any given point in the time–temperature domain until the end of the associating process,[1] the system should consist of the solvent and two 'groups' of agar molecules. The first group contains those agar molecules that are not associated with any others. The rheological behavior of these free agar molecules is theorized to be described by the adapted Rouse model which includes the temperature dependence of $\zeta_0(\tau)$ as proposed above. These free molecules need not be random coils throughout the whole time–temperature domain that they are available. Their departure from the

[1] Note that strictly speaking we cannot define an end of gelation due to aging and relaxing effects.

random coil conformation and the associated change in the value of $S(T)$ has been lumped into the $\zeta_0(T)$ term as described above (Eqs. (20) and (21)).

The second group of agar molecules contains the molecules that are associated with at least one other partner, forming helices and suprafibers and/or physical entanglements. The rheological behavior of this group will be based on the model of crosslinked polymers, as developed by Mooney (1959) (Eqs. (16)–(19)).

Since no chemical polymerization takes place, the total number of agar molecules remains the same:

$$n + n_{\text{assoc}} = n_{\text{total}} \tag{24}$$

where n is the number of non-associated agar molecules per unit volume, n_{assoc} is the number of associated molecules per unit volume, and n_{total} is the total number of agar molecules per unit volume.

3.3. Gelation equation

Previous studies have illustrated the effect of cooling rate on the microstructure and the rheological and mechanical properties of agar gels (Kusukawa et al., 1999; Labropoulos, 2001; Lee et al., 1997; Mohammed et al., 1998a). It was shown that a high cooling rate, such as that obtained by rapid quenching from a temperature above T_{gel} to a temperature well below T_{gel}, results in a gel microstructure with an average pore diameter smaller than that obtained by slow cooling. In real applications, such as PIM, the time–temperature profiles are rather complex and therefore a model that can utilize time and temperature data instead of fixed values of cooling rates is desirable.

Time, t, and temperature, T, are in fact separable variables. Temperature will affect the association rate. For a given association rate, time will then control how gelation will proceed to completion. Let $t = 0$ be the moment when $T = T_{\text{gel}}^{\text{model}}$. Taking into account the presence of clusters, at $t = 0$ we will have two groups:

$$0 < n^0 < n_{\text{total}} \qquad \text{non-associated agar molecules m}^{-3} \tag{25}$$

$$0 < n^0_{\text{assoc}} < n_{\text{total}} \qquad \text{associated agar molecules m}^{-3} \tag{26}$$

At $t > 0$, the rate of association, $\mathrm{d}n_{\text{assoc}}/\mathrm{d}t$, should depend on the available concentration of non-associated molecules, n. The rate should also be affected by the presence of the agar network that has already been developed. It is theorized that the higher the number of associated molecules and the denser the developed network, the higher the probability that a non-associated molecule will associate with the existing network. Due to the random processes that take place during gelation, it is very difficult to predict how a three-dimensional network will evolve and how it will affect the rate of association. However, to a first approximation, the rate of association should be proportional to the number of associated molecules, n_{assoc} per unit volume. We can therefore approximate the gelation equation as follows:

$$\frac{\mathrm{d}n_{\text{assoc}}}{\mathrm{d}t} = \xi(T) n_{\text{assoc}} n = \xi(T) n_{\text{assoc}} (n_{\text{total}} - n_{\text{assoc}}) \Rightarrow \frac{\mathrm{d}n_{\text{assoc}}}{\mathrm{d}t} = \xi(T) n_{\text{total}} \left(1 - \frac{n_{\text{assoc}}}{n_{\text{total}}}\right) n_{\text{assoc}} \tag{27}$$

Labropoulos (2001) has shown that this approximation (Eq. (27)) can be derived using the concept of agar-strand-equivalents. Eq. (27) has the form of the Verhulst or logistics equation and can be solved subject to the initial condition $0 < n^0_{\text{assoc}} < n_{\text{total}}$ (Eq. (26)) as follows:

$$n_{\text{assoc}} = \frac{n^0_{\text{assoc}} n_{\text{total}}}{n^0_{\text{assoc}} + (n_{\text{total}} - n^0_{\text{assoc}}) \mathrm{e}^{-rt}} \tag{28}$$

where $r = \xi(T) n_{\text{total}}$ is the net intrinsic association rate ($r = r_{\text{association}} - r_{\text{disassociation}}$), and is dependent on temperature.

The temperature dependence of the net intrinsic association rate $r(T)$ is proposed to have the following empirical form (for brevity T_{gel} is substituted for $T_{\text{gel}}^{\text{model}}$, except as noted otherwise):

$$r(T) = A_1 \underbrace{\left(\frac{T_{\text{ref}} - T_{\text{low}}}{T - T_{\text{low}}}\right)^{A_2}}_{\text{Mobility term}} \underbrace{\left(\frac{T_{\text{gel}} - T}{T_{\text{gel}} - T_{\text{low}}}\right)^{A_3}}_{\text{Driving force term}} \qquad T_{\text{low}} < T < T_{\text{gel}} \tag{29}$$

where A_1 is the maximum reaction rate attained between T_{gel} and T_{low}, A_2 was described in Eq. (20), and A_3 is a power exponent with a similar function as A_2. Note that Eq. (29) predicts that the association rate will be zero at T_{gel} (due to the absence of a driving force) and at T_{low} (due to zero mobility: mobility is inversely proportional to ζ_0 (Rouse, 1953) and tends to zero as temperature tends to T_{low}). While the form of Eq. (29) is satisfactory for the purpose of this study, the behavior of the association rate may be more complex than that proposed here. In particular, both the mobility and driving force terms of the above equations may be time dependent also, signifying the effect of the evolving network on the mobility of the non-associated molecules and their probability of association. Such issues will, however, be addressed in future work.

3.4. Rheological behavior at infinite time

When the temperature is lowered well below T_{gel} and after infinite time, the dynamic moduli are essentially independent of frequency (Labropoulos et al., 2001; Lapasin & Pricl, 1995; Manno et al., 1999; Mohammed et al., 1998a; Mohammed, Hember, Richardson, & Morris, 1998b; Mohammed, Hember, Richardson, & Morris, 1998c; Olhero et al., 2000). The network strands are more rigid (solid-like behavior), compared with the more flexible state (liquid-like behavior) at higher temperatures or at the early stages of gelation (Manno et al., 1999; Mohammed et al., 1998a). These equilibrium values of the dynamic moduli ($G'_{\text{e}}, G''_{\text{e}}$)

are dependent on the thermal history of the gel (Labropoulos et al., 2001; Mohammed et al., 1998a) and the agar concentration (Labropoulos et al., 2001; Olhero et al., 2000).

As indicated in the literature (Lapasin & Pricl, 1995; Mohammed et al., 1998a; Normand et al., 2000; Ramzi et al., 1998), at agar concentrations above 1 wt%, the $\log(G'_e)$ vs. $\log(c)$ (where c is the agar concentration) curve has a slope of approximately 2, indicating a c^2 dependence of the asymptotic equilibrium modulus. Below 1 wt% the slope gradually changes to a much larger value (Lapasin & Pricl, 1995). However, when the sol is quenched from a temperature above T_{gel} to a very low value (e.g. 5 °C), the slope is approximately the same throughout most of the concentration range, and has a value greater than 2 (Mohammed et al., 1998a).

The value of the equilibrium dynamic storage modulus, G'_e, that is obtained at low temperatures after the end of gelation can be related to the equilibrium shear modulus, G_e, as predicted by rubber elasticity (Ferry, 1980; Flory et al., 1959; Mooney, 1959; Tobolsky et al., 1961). In Mooney's (1959) theory (Eqs. (16)–(19)), however, no equilibrium loss modulus is predicted. This is due to each strand in crosslinked polymers consisting of only one molecular chain in the random coil conformation; the contribution from each strand to the loss modulus is described by the Rouse theory.

In agar gels, however, each suprafiber consists of a large number of double helices. Obviously, the molecules do not have a random coil conformation when in this state. The factor Φ in Mooney's model takes account of the fact that the molecules are extended. Nevertheless, it may not be adequate to relate to the different mechanisms of energy storage and dissipation in agar gels at low temperatures, which are probably associated with a combination of bending and stretching of the semirigid structural units (suprafibers) (Ferry, 1980).

3.5. Frequency dependence of the dynamic moduli at T_{gel}, $T_{gel} - dT$ and $T_{gel} + dT$

As mentioned above, the dynamic moduli of agar gels are largely independent of frequency at low temperatures after completion of gelation. However, this is not the case at the early stages of gelation or at temperatures close to T_{gel} (Manno et al., 1999; Ross-Murphy, 1994). In the case of dilute biopolymer solutions, or agar sols at high temperatures, $G' \propto \omega, G'' \propto \omega^2$ and $G'' \geqslant G'$ except for the very high frequency region where a G'–G'' crossover may exist (Ross-Murphy, 1994). At very low concentrations and high oscillatory frequencies, both G' and G'' have a common slope (Manno et al., 1999; Ross-Murphy, 1994).

In the vicinity of T_{gel}, a plateau region may be observed (Ross-Murphy, 1994). Dynamic rheological measurements at conditions close to the T_{gel} are very difficult to perform. Manno et al. (1999) monitored the viscoelastic spectra of a 2 wt% agarose gel quenched to 46.5 °C. At 20 min after quenching, they indicated the presence of a plateau in the region of $0.1 < \omega < 10$ rad s^{-1}. Above $\omega \approx 10$ rad s^{-1}, the moduli (G' and G'') increased with frequency. The viscoelastic spectrum was proposed to be characteristic of entangled polymers with a short relaxation time of about 0.1 s and a repetition time lower than 10 s (Manno et al., 1999).

These observations indicate contributions to the dynamic moduli from the two groups of agar molecules mentioned above: the associated agar molecules that form the network and the non-associated agar molecules. As was discussed earlier, the non-associated agar molecules are proposed to have a Rouse-like behavior with increasing relaxation times as temperature is lowered, to reflect the changing surroundings they encounter. The dynamic moduli contributions of the non-associated molecules should decrease as their number, n, decreases with time. The elimination of the frequency dependent portion of the viscoelastic spectrum with increasing gelation time is partially attributed to the reduction in the number of the non-associated molecules.

It should be realized that, regarding the network contributions, during the initial stages of gelation the network is rather flexible. This is supported by the theory of *entropic elasticity* and *enthalpic elasticity* (Ramzi et al., 1998). Entropic elasticity involves flexible objects. In the case of agar networks at the early stages of gelation, the flexible entities are the suprafibers and their disordered junctions. Let ψ represent the angle between two helices, each belonging to different suprafibers. If, during a deformation, the angle between the helices changes, $\langle \delta\psi^2 \rangle \neq 0$, i.e. the network is flexible, the network properties are governed by entropic elasticity (Ramzi et al., 1998). When the network is totally rigid, i.e. $\langle \delta\psi^2 \rangle \neq 0$, the network properties are governed by enthalpic elasticity. At the initial stages of gelation the rigidity of the suprafibers is low. However, their flexibility decreases as more agar molecules are attached. At later stages of gelation, any flexibility in the network will be associated with the degree of disorder in the junction regions.

The flexibility of the network influences the frequency dependence of the network contributions to the dynamic moduli of the system. With decreasing flexibility, the relaxation times of the suprafibers and the junctions are shifted progressively to higher values as gelation proceeds.

Similar to the discussion in Section 3.4, there should exist equilibrium moduli terms ($G'_e(n^0_{assoc}), G''_e(n^0_{assoc})$) with values lower than those of the asymptotic equilibrium moduli, G'_e and G''_e. At the very initial stages of gelation ($t \approx 0$) the formed network resembles that of a crosslinked polymer, however, due to the presence of the suprafibers (even at their initial stages), each of which containing more than one molecule, the frequency dependence of the network may not be comparable with that of the Mooney model. Instead, it is proposed that the dynamic moduli at $T = T_{gel}$ and $t = 0$ or at $T = T_{gel} - dT$ and $t = dt$ could be

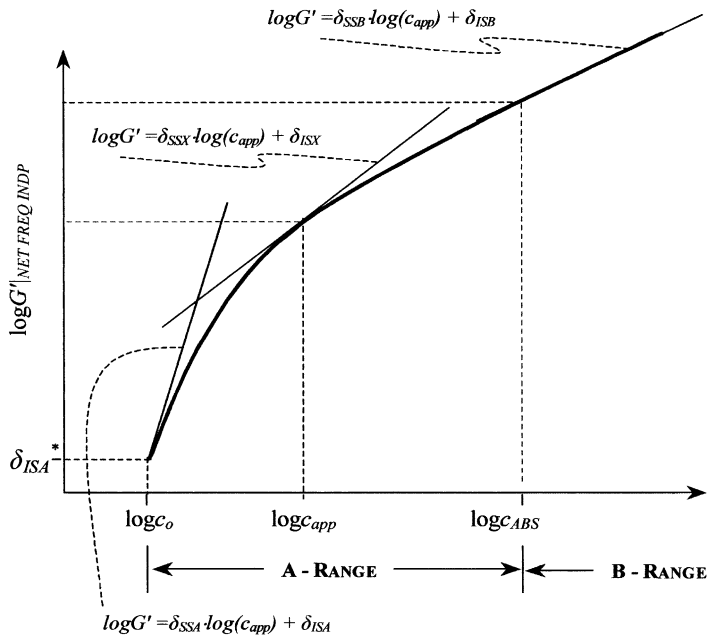

Fig. 3. Proposed apparent concentration dependence (log c_{app}) of the frequency independent contributions from the associated molecules to the storage modulus, $G'|^{c,t,T}_{\text{NET FREQ INDP}}$. Similar behavior is theorized for the frequency independent contributions from the associated molecules to the viscous modulus, $G''|^{c,t,T}_{\text{NET FREQ INDP}}$, where δ_{SSA}, δ_{SSB}, δ_{ISB} and δ_{ISA} are substituted with δ_{SVA}, δ_{SVB}, δ_{IVB} and δ_{IVA}, respectively. Apparent concentration is $c_{\text{app}} = n_{\text{assoc}}c/n_{\text{total}}$, where c is the total agar concentration in wt%.

approximated by

$$G'|^{\mathrm{d}t}_{\text{network}} = G'_{\text{e}}(n_{\text{assoc}}0) + n^0_{\text{assoc}}kT_{\text{gel}}\delta_{\text{FSA}}(\omega,T) \tag{30}$$

$$G''|^{\mathrm{d}t}_{\text{network}} = G''_{\text{e}}\left(n^0_{\text{assoc}}\right) + n^0_{\text{assoc}}kT_{\text{gel}}\delta_{\text{FVA}}(\omega,T) \tag{31}$$

where $G'_{\text{e}}(n^0_{\text{assoc}})$ and $G''_{\text{e}}(n^0_{\text{assoc}})$ are the values of the frequency independent parts of the network contributions to the respective dynamic moduli. Note the presence of an equilibrium term $G''_{\text{e}}(n^0_{\text{assoc}})$ for the loss modulus contributions of the associated molecules. This equilibrium term reflects the dissipation of energy associated with the presence of multi-unit suprafibers. Both $G'_{\text{e}}(n^0_{\text{assoc}})$ and $G''_{\text{e}}(n^0_{\text{assoc}})$ are dependent on the number of associated molecules (which at $t = \mathrm{d}t$ is equal to n^0_{assoc}). The functions δ_{FSA} and δ_{FVA} are related to the microstructure and are dependent on the applied oscillatory frequency and the thermal history of the sol.

At temperatures slightly above T_{gel} where no continuous network exists, the frequency independent terms of the above equations should vanish. Nevertheless, as discussed earlier, at temperatures close to and above T_{gel}, it is theorized that clusters exist which contribute to the viscoelastic behavior of the whole system. The rheological behavior of these entities could be based on theories developed for rigid molecules (Bixon & Zwanzig, 1978; Lai & Lii, 1997; Warren et al., 1973) and for branched flexible random coils (Ferry, 1980).

In these theories, a rotational relaxation time is introduced which is a measure of the time required for end-over-end rotation of the rigid molecule. If the clusters are assumed to have a rotational relaxation time, τ_0, then their viscoelastic functions right before $t = 0$ (i.e. $T = T_{\text{gel}} + \mathrm{d}T$) could be approximated as follows:

$$G'|^{t\approx 0}_{\text{clusters}} = n^0_{\text{assoc}}kT_{\text{gel}}\left(\frac{\delta_{\text{FSC1}}(T)\omega^2\tau_0^2}{1+\omega^2\tau_0^2} + \delta_{\text{FSC2}}(\omega,T)\right) \tag{32}$$

$$G''|^{t\approx 0}_{\text{clusters}} = n^0_{\text{assoc}}kT_{\text{gel}}\left(\frac{\delta_{\text{FVC1}}(T)\omega\tau_0}{1+\omega^2\tau_0^2} + \delta_{\text{FVC2}}(\omega,T)\right) \tag{33}$$

where $\delta_{\text{FSC1}}(T)$ and $\delta_{\text{FVC1}}(T)$ are temperature dependent parameters related to the rotation of the clusters, respectively, as applied to the clusters' contributions to the storage and viscous moduli of the system. The functions $\delta_{\text{FSC2}}(\omega,?)$ and $\delta_{\text{FVC2}}(\omega,T)$ are related to the internal structure of the clusters and describe the frequency dependence of the storage and viscous moduli of the clusters, respectively. As in the case with δ_{FSA} and δ_{FVA}, the form of these frequency dependent functions is not known and is very difficult to estimate from the available data. The number of clusters per unit volume (approximately proportional to n^0_{assoc}, assuming similar structure for all clusters) is effectively lumped into the parameters δ_{FSC1} and δ_{FVC1} and the functions δ_{FSC2} and δ_{FVC2}.

3.6. Transition from T_{gel} to T_{low}

Various studies have shown the effect of the thermal history of the gel on the values of the equilibrium dynamic moduli (Labropoulos et al., 2001; Manno et al., 1999; Mohammed et al., 1998a), the quality of the final gel

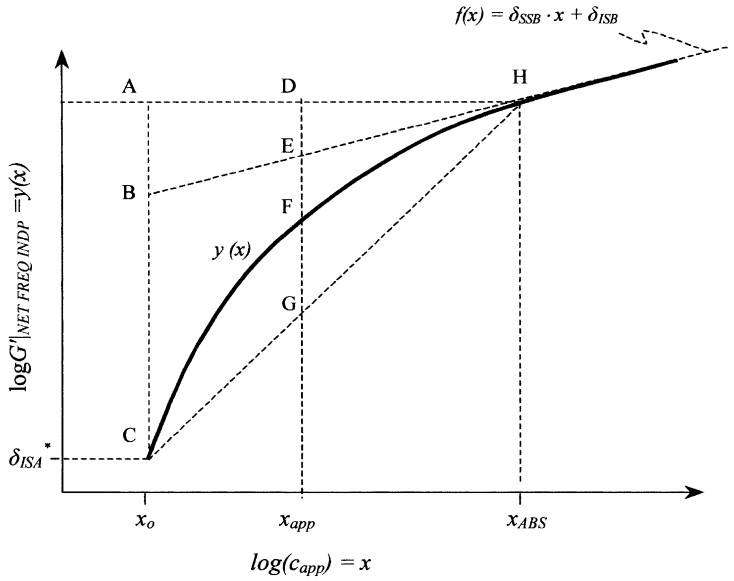

Fig. 4. Schematic for an empirical approximation of $\log G'|^{c,t,T}_{\text{NET FREQ INDP}} = y(x)$ at an apparent concentration $\log(c_{\text{app}}) = x$ within the range $\log(c_0) = x_0$ and $\log(c_{\text{ABS}}) = x_{\text{ABS}}$. Line BEH is given by the equation: $y(x) = \delta_{\text{SSB}}x + \delta_{\text{ISB}}$ and the value of $y(x_0)$ is denoted by δ^*_{ISA}. See text for more detailed explanation.

microstructure (Kusukawa et al., 1999; Labropoulos, 2001; Lee et al., 1997; Mohammed et al., 1998a), the gel's mechanical properties (Lee et al., 1997) and the gel's melting behavior (Mohammed et al., 1998a). To a first approximation, and for the scope of this study, it can be assumed that the dependence of the dynamic moduli on the number of associated molecules is comparable for a wide range of cooling rates. In effect, this assumption allows us to have the same form of equations describing the dynamic moduli for a wide range of cooling patterns as a function of the number of associated molecules.

Another fundamental assumption is that the effect of n_{assoc} on the frequency independent part of the dynamic moduli of the evolving network (termed, respectively, $G'|^{c,t,T}_{\text{NET FREQ INDP}}$ and $G''|^{c,t,T}_{\text{NET FREQ INDP}}$) is similar to the concentration dependence (Mohammed et al., 1998a) of the equilibrium dynamic moduli, G'_{e} and G''_{e}. In effect, it is theorized that at any given time $t > 0$ the values of $G'|^{c,t,T}_{\text{NET FREQ INDP}}$ and $G''|^{c,t,T}_{\text{NET FREQ INDP}}$ will be equal to the values of the equilibrium dynamic moduli, $G'_{\text{e}}(c_{\text{app}})$ and $G''_{\text{e}}(c_{\text{app}})$ at an apparent concentration $c_{\text{app}} = n_{\text{assoc}}c/n_{\text{total}}$, where c is the total agar concentration in wt%.

Fig. 3 illustrates this concept. Above an apparent concentration, $c_{\text{app}} > c_{\text{ABS}}$, the $\log G'|^{c,t,T}_{\text{NET FREQ INDP}}$ vs. $\log(c_{\text{app}})$ curve becomes linear and can be approximated by a straight line:

$$\log G'|^{c,t,T}_{\text{NET FREQ INDP}} = \delta_{\text{SSB}} \log \frac{n_{\text{assoc}}c}{n_{\text{total}}} + \delta_{\text{ISB}} \tag{34}$$

In the range between $c_0 = n^0_{\text{assoc}}c/n_{\text{total}}$ and c_{ABS} (termed A-range), the slope δ_{SSX} of the $\log G'|^{c,t,T}_{\text{NET FREQ INDP}}$ vs. $\log(c_{\text{app}})$ curve at any c_{app} will be gradually decreasing with increasing c_{app}. The upper limiting value of the slope, δ_{SSX}, will be δ_{SSA} at an apparent concentration c_0. The lower limiting value of δ_{SSX} will be δ_{SSB} at an apparent concentration c_{ABS}.

A similar approach can be employed for the frequency independent network contributions to the dynamic viscous modulus. The parameters' terminology is changed accordingly. The following equations describe the contributions to the dynamic moduli from the associated molecules for the temperature range $T_{\text{low}} < T < T_{\text{gel}}$:

Dynamic storage modulus: (A-range), i.e. $n^0_{\text{assoc}} < n_{\text{assoc}} < (c_{\text{ABS}} \times 10^4 N_{\text{A}}/M)$

$$G'|^{c,t,T}_{\text{associated}} = G'|^{c,t,T}_{\text{NET FREQ INDP}} + n_{\text{assoc}}kT\delta_{\text{FSA}} \tag{35}$$

$$\log G'|^{c,t,T}_{\text{NET FREQ INDP}} = \delta_{\text{SSX}} \log \frac{n_{\text{assoc}}c}{n_{\text{total}}} + \delta_{\text{ISX}} \tag{36}$$

$$\delta_{\text{SSB}} \le \delta_{\text{SSX}} \le \delta_{\text{SSA}} \tag{37}$$

$$\delta_{\text{ISA}} \le \delta_{\text{ISX}} \le \delta_{\text{ISB}} \tag{38}$$

Dynamic storage modulus: (B-range), i.e. $(c_{\text{ABS}}10^4 N_{\text{A}}/M) < n_{\text{assoc}} < n_{\text{total}}$

$$G'|^{c,t,T}_{\text{associated}} = G'|^{c,t,T}_{\text{NET FREQ INDP}} + n_{\text{assoc}}kT\delta_{\text{FSB}} \tag{39}$$

$$\log G'|^{c,t,T}_{\text{NET FREQ INDP}} = \delta_{\text{SSB}} \log \frac{n_{\text{assoc}}c}{n_{\text{total}}} + \delta_{\text{ISB}} \tag{40}$$

Dynamic viscous modulus: (A-range): $n^0_{\text{assoc}} < n_{\text{assoc}} < (c_{\text{ABV}}10^4 N_{\text{A}}/M)$

$$G''|^{c,t,T}_{\text{associated}} = G''|^{c,t,T}_{\text{NET FREQ INDP}} + n_{\text{assoc}}kT\delta_{\text{FVA}} \tag{41}$$

$$\log G''|^{c,t,T}_{\text{NET FREQ INDP}} = \delta_{\text{SVX}} \log \frac{n_{\text{assoc}}c}{n_{\text{total}}} + \delta_{\text{IVX}} \tag{42}$$

$$\delta_{\text{SVB}} \le \delta_{\text{SVX}} \le \delta_{\text{SVA}} \tag{43}$$

Table 1
Description of parameters and functions used in Eqs. (35)–(49)

Name	Description
c_{ABS}	Agar concentration in wt%, signifying transition from *A* to *B*-range for the network contributions to G'
c_{ABV}	Agar concentration in wt%, signifying transition from *A* to *B*-range for the network contributions to G''
c_{app}	Apparent concentration: $c_{app} = n_{assoc}c/n_{total}$
c_0	Critical gelling concentration: $c_0 = n^0_{assoc}c/n_{total}$
c	Total agar concentration in wt%
$G'\|^{c,t,T}_{\text{NET FREQ INDP}}$	Frequency independent contributions to G' from the network
$G''\|^{c,t,T}_{\text{NET FREQ INDP}}$	Same as above but for G''
δ_{SSA}	Slope of the tangent (Eq. (36)) to the $\log G'\|^{c,t,T}_{\text{NET FREQ INDP}}$ vs. $\log c_{app}$ curve at c_0
δ_{ISA}	Intercept of the tangent (Eq. (36)) to the $\log G'\|^{c,t,T}_{\text{NET FREQ INDP}}$ vs. $\log c_{app}$ line at c_0 $= \delta_{SSA} \log c_0 + \delta_{ISA}$
δ^*_{ISA}	
δ_{SSB}, δ_{ISB}	Same as δ_{SSA} and δ_{ISA}, respectively, but at c_{ABS}
δ_{SVA}, δ_{IVA}	Same as δ_{SSA} and δ_{IVA} but for G''
δ^*_{IVA}	$= \delta_{SVA} \log c_0 + \delta_{IVA}$
δ_{SVB}, δ_{IVB}	Same as δ_{SVA} and δ_{IVA}, respectively, but at c_{ABV}
us, *uv*	*us* is used in Eq. (48) that controls the curvature of the curve in Fig. 4. Similar function for *uv* (Eq. (49))
δ_{FSA}, δ_{FSB}	Functions describing the frequency dependence of $G'\|_{assoc}$ in *A*, *B* ranges, respectively
δ_{FVA}, δ_{FVB}	Functions describing the frequency dependence of $G''\|_{assoc}$ in *A*, *B* ranges, respectively

$$\delta_{IVA} \le \delta_{IVX} \le \delta_{IVB} \tag{44}$$

Dynamic viscous modulus: (*B*-range): $(c_{ABV}10^4 N_A/M) < n_{assoc} < n_{total}$

$$G''|^{c,t,T}_{\text{associated}} = G''|^{c,t,T}_{\text{NET FREQ INDP}} + n_{assoc}kT\delta_{FVB} \tag{45}$$

$$\log G''|^{c,t,T}_{\text{NET FREQ INDP}} = \delta_{SVB} \log \frac{n_{assoc}c}{n_{total}} + \delta_{IVB} \tag{46}$$

One of the practical problems in obtaining the curve in Fig. 3 is how one can describe the apparent concentration dependence of the slopes δ_{SSX}, δ_{SVX} and the intercepts δ_{ISX}, δ_{IVX}, within the range c_0 and c_{ABS}. In fact, such functions, $\delta_{SSX}(c_{app})$ and $\delta_{ISX}(c_{app})$ for G' and the respective ones for G'', $\delta_{SVX}(c_{app})$ and $\delta_{ISX}(c_{app})$ would probably introduce more parameters in addition to the limiting values δ_{SSA}, δ_{ISA}, δ_{SSB}, δ_{ISB}, δ_{SVA}, δ_{IVA}, δ_{SVB}, and δ_{IVB}.

The problem is circumvented by using an empirical approach in which the value of $\log G'|^{c,t,T}_{\text{NET FREQ INDP}}$ is estimated as shown in Fig. 4. For brevity $y(x)$ and x are substituted for $\log G'|^{c,t,T}_{\text{NET FREQ INDP}}$ and $\log(c_{app})$, respectively. Similarly, the limiting values for $\log(c_{app})$ become x_0 and x_{ABS}.

The value of the curve $y(x)$ at x_{app}, i.e. $y(x_{app})$, will correspond to point *F* and is denoted as $y_F(x)$ (the subscript denotes the point we refer to). The values of $y(x)$ at x_0 and x_{ABS} will be $y_C(x)$ and $y_H(x)$, respectively.

Point *H* can be calculated by the tangent line $f(x) = \delta_{SSB}x + \delta_{ISB}$ (i.e. $\log G' = \delta_{SSB} \log(c_{app}) + \delta_{ISB}$) at x_{ABS}. Point *C*, which corresponds to the value of $y(x)$ at x_0, can be calculated by the tangent to the curve at that point, i.e. $g(x) = \delta_{SSA}x + \delta_{ISA}$. In practice though, the value is denoted by δ^*_{ISA} to reduce the number of parameters used ($y_C(x) = \delta^*_{ISA} = \delta_{SSA} \log(c_0) + \delta_{ISA}$). The value of the curve $y(x)$ at point *F*, i.e. $y_F(x)$, can be approximated by using points *D*, *E* and *G* as follows:

$$y_F(x) = f_E(x) - EF \Rightarrow y_F(x) = f_E(x) - \left(\frac{x_{ABS} - x}{x_{ABS} - x_0}\right)^{us} EG \tag{47}$$

where the length of the segment *EF* is empirically approximated as shown in the earlier equation, with the introduction of the parameter *us*. If the parameter *us* is positive, the curve segment *CFH* lies above the line *CGH*. If the parameter *us* is equal to zero then the segment *CFH* coincides with line CGH. If the parameter *us* is negative, the curve segment *CFH* lies below the line *CGH*. The magnitude of *us* controls the shape of the curve; $us = \infty$ corresponds to segment *CBEH*. The length of segment *EG* can be given by $(BC \times DE)/AB$ so that Eq. (47) becomes:

$$\log G' = y_F(x) = f_E(x) - \left(\frac{x_{ABS} - x}{x_{ABS} - x_0}\right)^{us} \frac{BC}{AB} DE$$

$$= f_E(x) - \left(\frac{x_{ABS} - x}{x_{ABS} - x_0}\right)^{us} \frac{\delta_{SSB}x_0 + \delta_{ISB} - \delta^*_{ISA}}{\delta_{SSB}(x_{ABS} - x_0)} \times (\delta_{SSB}(x_{ABS} - x_{app})) \tag{48}$$

where $f_E(x) = \delta_{SSB}x_{app} + \delta_{ISB}$ is the tangent line to the curve at x_{ABS} and effectively the equation of the curve $y(x)$ at $x_{app} \ge x_{ABS}$ (i.e. *B*-range, Fig. 3).

The apparent concentration dependence of $G''|^{c,t,T}_{\text{NET FREQ INDP}}$ is treated similarly with the appropriate notation of parameters (i.e. introduction of the exponent *uv*, and the parameter $\delta^*_{IVA} = \delta_{SVA} \log(c_0) + \delta_{IVA}$) :

$$\log G'' = h_F(x) = j_E(x)$$

$$-\left(\frac{x_{ABV} - x}{x_{ABV} - x_0}\right)^{uv} \frac{\delta_{SVB}x_0 + \delta_{IVB} - \delta^*_{IVA}}{\delta_{SVB}(x_{ABV} - x_0)} \times (\delta_{SVB}(x_{ABV} - x_{app})) \tag{49}$$

where $j_E(x) = \delta_{SVB}x_{app} + \delta_{IVB}$. A brief explanation of the parameters used in the earlier equations is given in Table 1. As mentioned earlier, the contributions to the dynamic moduli from the *free* molecules will be described by the Rouse model (Eqs. (5)–(7)) where $n = n_{total} - n_{assoc}$.

3.7. Transition from T_{ref} to T_{gel}

The solution of the gelation equation required the presence of a minimum number of associated molecules, n^0_{assoc}. This number was related to the presence of clusters. At a temperature slightly above T_{gel} it was proposed that their contributions to the dynamic moduli of the system, would be given by Eqs. (32) and (33).

Since it is difficult to obtain accurate dynamic rheological

data in this temperature range, it is proposed that Eqs. (32) and (33) also hold for the clusters' contributions above T_{gel}, with the exception that n^0_{assoc} is replaced by $n_{clusters}$, which is the number of agar molecules per unit volume that participate in cluster formation. The upper limiting value of this $n_{clusters}$ is n^0_{assoc}, whereas at high temperatures $n_{clusters}$ should vanish to zero. A simple empirical formula for $n_{clusters}$, which does not introduce any additional fitting parameters, is the following:

$$n_{clusters} = n^0_{assoc}\left(1 - \frac{T - T_{gel}}{373.15 - T_{gel}}\right)^{1/2} \quad (50)$$

In reality, the functions $\delta_{FSC2}(\omega,?)$ and $\delta_{FVC2}(\omega,T)$ should change also, becoming less frequency dependent as temperature is lowered from T_{ref} to T_{gel}. Lack of data in this temperature range precludes any assumptions about the behavior of $\delta_{FSC2}(\omega,?)$ and $\delta_{FVC2}(\omega,T)$.

4. Summary

The proposed rheological model builds on the characteristic features of agar gels. Initially, at high temperatures, agar molecules take on a random coil conformation. As gelation proceeds, the agar molecules associate with each other forming double helices and higher order assemblies termed suprafibers. These entities have different rheological behavior and their relative contributions to the gel system changes with time and temperature.

The contributions from the non-associated molecules are theorized to be approximated by an adapted Rouse model, in which the monomeric friction coefficient, ζ_0, increases with decreasing temperature and accounts for the shift of the relaxation spectrum towards higher values. It tends to infinity as temperature approaches a low limiting value in the vicinity of the freezing point.

The contributions from associated molecules can be classified into two categories. The first category consists of the associated molecules that form clusters of molecules. These clusters are not interconnected to each other, thus, the creation of a continuous three-dimensional network (with a corresponding solid-like behavior) is not possible. The rheological behavior of these clusters is based on the theory for partially flexible helical macromolecules. An end-to-end rotational relaxation time is predicted as well as a frequency dependence term arising from the internal network of the clusters.

A theoretical gelation temperature, T^{model}_{gel} is defined as the temperature at which the clusters form a continuous three-dimensional network for the first time. Below T^{model}_{gel} the rheological behavior of agar gel is dominated by the contributions from the evolving network. These associated molecules form the second category. The network is initially compliant, thus its contributions to the dynamic moduli of the system include a frequency dependent term. There also exist frequency independent terms (for both G' and G'') that relate to the ability of the evolving network to store and dissipate energy, with a solid-like behavior. The frequency dependence of the network gradually disappears as more and more agar molecules associate and increase the stiffness of the network. Eventually when all agar molecules associate, the network will reach equilibrium moduli values, G'_e and G''_e that are dependent on agar concentration and the thermal history.

The dependence of the frequency independent contributions of the dynamic moduli on the fraction of associated molecules is proposed to be similar to the concentration dependence of the equilibrium moduli G'_e and G''_e. These contributions increase with increasing number of associated molecules.

The gelation equation is approximated by the Verhulst equation, assuming that the association rate is proportional to the number of non-associated agar molecules, n and the number of associated agar molecules (in the form of a network) n_{assoc}. The gelation equation includes a temperature dependent intrinsic association rate, $r(T)$, that increases as the temperature is lowered in the range between T^{model}_{gel} and T_{low}. The gelation equation allows the calculation of the number of non-associated agar molecules, n, and the number of associated agar molecules, n_{assoc} and thus the individual contributions to the dynamic moduli from all entities present during the gelation process.

The proposed model includes the effect of thermal history on the rheological behavior of agar gels through appropriate adaptation of the model parameters. The estimation of the values of the model parameters as a function of agar concentration and cooling rate is the subject of Part II of this study where the proposed model is fitted to experimental gelation curves prepared under a wide range of gelation conditions.

Acknowledgements

This project was sponsored by the Malcolm G. McLaren Center for Ceramic Research, Rutgers University, and PowderFlow™ Technologies, Honeywell Int.

References

Amici, E., Clark, A. H., Normand, V., & Johnson, N. B. (2000). *Biomacromolecules*, *1*, 721.
Aplin, J. D., & Hall, L. D. (1979). *Carbohydrate Research*, *75*, 17.
Araki, C. (1944a). *Journal of Chemistry Japan*, *65*, 533.
Araki, C. (1944b). *Journal of Chemistry Japan*, *65*, 627.
Araki, C. (1956). *Bulletin of the Chemical Society of Japan*, *29*, 43.
Araki, C., & Hirase, S. (1954). *Bulletin of the Chemical Society of Japan*, *27*, 109.
Arnott, S., Fulmer, A., Scott, W. E., Dea, I. C. M., Moorhouse, R., & Rees, D. A. (1974). *Journal of Molecular Biology*, *90*, 269.
Bixon, M., & Zwanzig, R. (1978a). *Journal of Chemical Physics*, *68*, 1896.
Bixon, M., & Zwanzig, R. (1978b). *Journal of Chemical Physics*, *68*, 1890.
Bueche, F. (1952). *Journal of Chemical Physics*, *20*, 1959.
Bulone, D., Emanuele, A., & San Biagio, P. L. (1999). *Biophysical Chemistry*, *77*, 1.

Cesarano III, J. PhD Dissertation, University of Washington, 1989.
Charlionet, R., Levasseur, L., & Malandain, J. -J. (1996). *Electrophoresis*, *17*, 58.
Dea, I. C. M., & Rees, D. A. (1987). *Carbohydrate Polymers*, *7*, 183.
Dea, I. C. M., McKinnon, A. A., & Rees, D. A. (1972). *Journal of Molecular Biology*, *68*, 153.
Falshaw, R., Furneaux, R. H., & Stevenson, D. E. (1998). *Carbohydrate Research*, *308*, 107.
Fanelli, A. J., Silvers, R. D., Frei, W. S., Burlew, J. V., & Marsh, G. B. (1989). *Journal of American Ceramic Society*, *72*, 1833.
Ferry, J. D. (1980). *Viscoelastic properties of polymers*, (3rd ed). New York: Wiley.
Flory, P. J., Hoeve, C. A. J., & Ciferri, A. (1959). *Journal of Polymer Science*, *34*, 337.
Gabrielson, L., & Edirisinghe, M. J. (1996). *Journal of Material Science Letters*, *15*, 1105.
Griess, G. A., Guiseley, K. B., & Serwer, P. (1993). *Biophysical Journal*, *65*, 138.
Griess, G. A., Edwards, D. M., Dumais, M., Harris, R. A., Renn, W., & Serwer, P. (1993). *Journal of Structural Biology*, *111*, 39.
Guiseley, K. B. (1970). *Carbohydrate Research*, *13*, 247.
Haga, H., Sasaki, S., Morimoto, M., Kawabata, K., Ito, E., Abe, K., & Sambongi, T. (1998). *Japanese Journal of Applied Physics*, *37*, 3860–3863.
Harris, P. (1990). *Food gels*, New York: Elsevier.
Hickson, T. G. L., & Polson, A. (1968). *Biochimica et Biophysica Acta*, *165*, 43.
Hirase, S. (1957). *Bulletin of the Chemical Society of Japan*, *30*, 75.
Kirkwood, J. G., & Auer, P. L. (1951). *Journal of Chemical Physics*, *19*, 281.
Kouwijzer, M., & Pérez, S. (1998). *Biopolymers*, *46*, 11.
Kratky, O., & Porod, G. (1949). *Recueil des Travaux Chimiques des Pays-Bas*, *68*, 1106.
Kusukawa, N., Ostrovsky, M. V., & Garner, M. M. (1999). *Electrophoresis*, *20*, 1455.
Labropoulos, K. C. PhD Dissertation, Rutgers University, 2001.
Labropoulos, K. C., Rangarajan, S., Niesz, D. E., & Danforth, S. C. (2000). Correlation of the dynamic rheological behavior and microstructure of agar gel based aqueous binders for powder injection molding. In N. Bansal & J. P. Singh, *Innovative processing and synthesis of ceramics glasses and composites IV. Ceramic Transactions* (pp. 161–172), Vol. 115.
Labropoulos, K. C., Rangarajan, S., Niesz, D. E., & Danforth, S. C. (2001). *Journal of American Ceramic Society*, *84* (6), 1217.
Lai, M. -F., & Lii, C. (1997). *Inernational Journal of Biological Macromolecules*, *21*, 123.
Lai, M. -F., Huang, A. -L., & Lii, C. (1999). *Food Hydrocolloids*, *13*, 409.
Lange, F. F. (1989). *Journal of American Ceramic Society*, *72*, 3.
Lapasin, R., & Pricl, S. (1995). *Rheology of industrial polysaccharides: Theory and applications*, London, UK: Blackie A and P.
Larson, R. G. (1988). *Constitutive equations for polymer melts and solutions*, Boston: Butterworks.
Lee, J. -P., Lee, K. -H., & Song, H. -K. (1997). *Journal of Material Science*, *32*, 5825.
Manno, M., Emanuele, A., Mantorana, V., Bulone, D., San Biagio, P. L., Palma-Vittoreli, B., & Plama, M. U. (1999). *Physical Review Letters E*, *59*, 2222.
Mitsuiki, M., Mizuno, A., & Motoki, M. (1999). *Journal of Agricultural Food Chemistry*, *47*, 473.
Mohammed, Z. H., Hember, M. W. N., Richardson, R. K., & Morris, E. R. (1998a). *Carbohydrate Polymers*, *36*, 15.
Mohammed, Z. H., Hember, M. W. N., Richardson, R. K., & Morris, E. R. (1998b). *Carbohydrate Polymers*, *36*, 27.
Mohammed, Z. H., Hember, M. W. N., Richardson, R. K., & Morris, E. R. (1998c). *Carbohydrate Polymers*, *36*, 37.
Mooney, M. (1959). *Journal of Polymer Science*, *34*, 599.
Nitta, T., Haga, H., Kawabata, K., Abe, K., & Sambongi, T. (2000). *Ultramicroscopy*, *82*, 223.
Normand, V., Lootens, D. L., Amici, E., Plucknett, K. P., & Aymard, P. (2000). *Biomacromolecules*, *1*, 730.
Norton, I. T., Jarvis, D. A., & Foster, T. J. (1999). *International Journal of Biological Macromolecules*, *26*, 255.
Nussinovitch, A., Velez-Silvestre, R., & Peleg, M. (2001). *Biotechnology Progress*, *9*, 101.
Oates, C. G., Lucas, P. W., & Lee, W. P. (1993). *Carbohydrate Polymers*, *20*, 189.
Olhero, S. M., Tarì, G., Coimbra, M. A., & Ferreira, J. M. F. (2000). *Journal of European Ceramic Society*, *20*, 423.
Ookubo, N., Komatsubara, M., Nakajima, H., & Wada, Y. (1976). *Biopolymers*, *15*, 929.
Pines, E., & Prins, W. (1973). *Macromolecules*, *6*, 888.
Ramzi, M., Rochas, C., & Guenet, J. -M. (1998). *Macromolecules*, *31*, 6106.
Rees, D. A. (1972). *Chemistry and Industry*, *8*, 630.
Ross-Murphy, S. B. (1994). *Physical techniques for the study of food biopolymers*, Glasgow: Blackie A and P.
Rouse, P. E. (1953). *Journal of Chemical Physics*, *21*, 1272.
Schafer, S. E., & Stevens, E. S. (1995). *Biopolymers*, *36*, 103.
Serwer, P. (1983). *Electrophoresis*, *4*, 375.
Tobolsky, A. V., Carlson, D. W., & Indictor, N. (1961). *Journal of Polymer Science*, *54*, 175.
Tsoegl, N. W. (1963). *Journal of Chemical Physics*, *39*, 149.
Tsoga, A., Kasapis, S., & Richardson, R. K. (1999). *Biopolymers*, *49*, 267.
Ullman, R. (1969). *Macromolecules*, *2*, 27.
Warren, T. C., Schrag, J. L., & Ferry, J. D. (1973). *Biopolymers*, *12*, 1905.
Whistler, R. L., & BeMiller, J. N. (1973). *Industrial gums*, New York: Academic.
Yamakawa, H. (1975). *Macromolecules*, *8*, 339.
Yamakawa, H., & Fujii, M. (1973). *Macromolecules*, *6*, 406.
Zimm, B. H. (1956). *Journal of Chemical Physics*, *24*, 269.